Journal of Peptide Science
J. Peptide Sci. **5**: 330–337 (1999)

Conformational Studies of a Bicyclic, Lactam-Constrained Parathyroid Hormone-Related Protein-Derived Agonist

ELISABETTA SCHIEVANO[a], STEFANO MAMMI[a], ALESSANDRO BISELLO[b], MICHAEL ROSENBLATT[b], MICHAEL CHOREV[b] and EVARISTO PEGGION[a,*]

[a] Department of Organic Chemistry, Biopolymer Research Center, University of Padova, Via Marzolo 1, Padova, Italy
[b] Division of Bone and Mineral Metabolism, Charles A. Dana and Thorndike Laboratories, Department of Medicine, Beth Israel Deaconess Medical Center and Harvard Medical School, Boston, USA

Received 5 January 1999
Accepted 26 March 1999

Abstract: The *N*-terminal 1–34 segments of both parathyroid hormone (PTH) and parathyroid hormone-related protein (PTHrP) bind and activate the same membrane receptor in spite of major differences in their amino acid sequence. The hypothesis was made that they share the same bioactive conformation when bound to the receptor. A common structural motif in all bioactive fragments of the hormone in water/trifluoroethanol mixtures or in aqueous solution containing detergent micelles is the presence of two helical segments at the *N*- and *C*-termini of the sequence. In order to stabilize the helical structures, we have recently synthesized and studied the PTHrP(1–34) analog [(Lys^{13}–Asp^{17}, Lys^{26}–Asp^{30})]PTHrP(1–34)NH$_2$, which contains lactam-constrained Lys-Asp side chains at positions i, $i+4$. This very potent agonist exhibits enhanced helix stability with respect to the corresponding linear peptide and also two flexible sites at positions 12 and 19 in 1:1 trifluoroethanol/water. These structural elements have been suggested to play a critical role in bioactivity. In the present work we have extended our conformational studies on the bicyclic lactam-constrained analog to aqueous solution. By CD, 2D-NMR and structure calculations we have shown that in water two helical segments are present in the region of the lactam bridges (13–18, and 26–31) with high flexibility around Gly^{12} and Arg^{19}. Thus, the essential structural features observed in the aqueous-organic medium are maintained in water even if, in this solvent, the overall structure is more flexible. Our findings confirm the stabilizing effect of side-chain lactam constraints on the α-helical structure. Copyright © 1999 European Peptide Society and John Wiley & Sons, Ltd.

Keywords: parathyroid hormone-related protein; conformational analysis; 2D-NMR; molecular dynamics

INTRODUCTION

Parathyroid hormone (PTH) is an 84-amino acid residue peptide that regulates extracellular calcium homeostasis [1]. The PTH-related protein (PTHrP) is a 141-amino acid residue protein, initially isolated as one of the factors involved in malignancy-associated hypercalcemia [1]. The sequence homology between PTH and PTHrP is concentrated in the *N*-terminal domain, where eight out of 13 residues are identical in the two hormones. After residue 13, the primary structures of the two hormones diverge completely. In spite of this difference in primary structures, the two hormones interact with the same seven transmembrane helix containing G-protein-coupled PTH/PTHrP receptor. It has also been shown that the *N*-terminal fragments 1–34 of both PTH and PTHrP retain the calciotropic activity of the intact hormones. Therefore, the hypothesis was made that the hormones share the same conformation when bound to the receptor [1]. Extensive studies carried

* Correspondence to: Department of Organic Chemistry, University of Padova, Via Marzolo 1, 35131 Padova, Italy. E-mail: Peggion@chor.unipd.it

Contract/grant sponsor: Consiglio Nazionale delle Ricerche (CNR); Contract/grant number: R01-DK47940

CCC 1075–2617/99/070330-08$17.50

out in different laboratories have shown that in water the conformation of the 1–34 fragments of the two hormones is essentially unordered, while an ordered structure is formed in H_2O/TFE (TFE, 2,2,2-trifluoroethanol) mixtures or in aqueous solutions containing detergent micelles [2–10]. The ordered conformation consists of two *N*- and *C*-terminal α-helical segments connected by a structurally ill-defined region. These structural motifs were assumed to be important elements for biological activity. Quite recently, we designed, synthesized and conformationally characterized a series of highly potent PTHrP(1–34)-based agonists and PTHrP(7–34)-based antagonists containing lactam-constrained side chains [3,4,11–13]. The lactam bridges connecting the side chains of Lys and Asp residues at positions i, $i+4$ were designed to enhance the stability of the helical segments at the *N*- and *C*-termini of the analogs. In particular, the agonist series [(Lys^{13}–Asp^{17},)]PTHrP(1–34)NH_2[(Lys^{26}–Asp^{30})]PTHrP(1–34)NH_2, [(Lys^{13}–Asp^{17}, Lys^{26}–Asp^{30})]-PTHrP(1–34)NH_2 was extensively investigated by combined 2D-NMR, distance geometry (DG) and molecular dynamics (MD) simulations in 1:1 TFE/H_2O [3]. The results indicated that the lactam constraints effectively favor the formation of the helical domains. The chiroptical properties revealed that the bis-lactam analog is 40% helical even in aqueous solution in the absence of the helix supporting solvent TFE [3]. This initial observation prompted the more detailed studies reported in this paper on the conformational preference of the highly potent bis-lactam analog: [(Lys^{13}–Asp^{17}, Lys^{26}–Asp^{30})]PTHrP(1–34)NH_2 in aqueous solution.

MATERIALS AND METHODS

Materials

The synthesis and the chemical and biological characterization of the agonist were reported elsewhere [11]. The pure peptide, recovered by lyophilization from the aqueous solution, contained some moisture. The peptide content of our sample, determined by quantitative amino acid analysis, was 68%. Milli-Q water was obtained by treating deionized water with a Millipore reagent grade water system. Tetramethylsilane (TMS) was purchased from Fluka AG.

Circular Dichroism

CD measurements in the range 185–250 nm were carried out at room temperature on a JASCO J-715 spectropolarimeter interfaced with a PC. Spectra were elaborated with a J-600 program for Windows. All experiments were carried out using quartz cells from Hellma with suprasil windows and with optical path lengths in the range 0.005–0.1 cm. The peptide concentration was in the range 10^{-3}–10^{-5} M. The spectra were recorded using a bandwidth of 2 nm, and a time constant of 4 s at a scan speed of 10

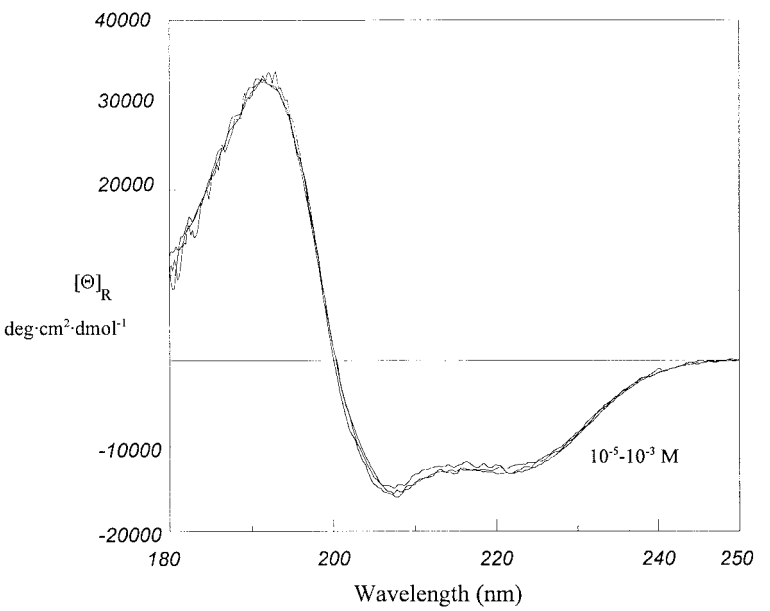

Figure 1 CD spectra of the bis-lactam analog in water, pH 4.5, at various concentrations (indicated).

Table 1 Proton chemical shifts (ppm), relative to TMS, of [(Lys^{13}–Asp^{17}, Lys^{26}–Asp^{30})]PTHrP(1–34)NH_2 in water

Residue	NH (ppm)	α (ppm)	β (ppm)	Other (ppm)
Ala^1		4.17	1.55	
Val^2	8.55	4.22	2.08	γ 0.97
Ser^3	8.52	4.49	3.86, 3.92	
Glu^4	8.56	4.31	1.98, 2.06	γ 2.43
His^5	8.59	4.64	3.19, 3.25	H_2 8.67, H_4 7.38
Gln^6	8.37	4.30	2.01, 2.06	γ 2.38, NH_2 6.92, 7.52
Leu^7	8.32	4.32	1.66	γ 1.59, δ_1 0.89, δ_2 0.92
Leu^8	8.18	4.28	1.65	γ 1.48, δ_1 0.87, δ_2 0.93
His^9	8.47	4.68	3.21, 3.33	H_2 8.67, H_4 7.39
Asp^{10}	8.40	4.68	2.85	
Lys^{11}	8.51	4.27	1.88, 1.94	γ_1 1.47, γ_2 1.51, δ 1.72, ε 3.03, NH_2 7.58
Gly^{12}	8.43	3.92, 3.97		
Lys^{13}	7.95	4.19	1.86, 1.92	γ_1 1.21, γ_2 1.38, δ_1 1.46, $\delta_2$1.62, ε_1 2.63, ε_2 3.70, NH 7.95
Ser^{14}	8.41	4.22	4.00	
Ile^{15}	7.70	3.96	1.92	γ_1 1.31, γ_2 1.59, $\gamma_{CH_3}+\delta_{CH_3}$ 0.97
Gln^{16}	8.05	4.08	2.14	γ 2.43, NH_2 7.51, 6.92
Asp^{17}	8.82	4.67	2.79, 2.87	
Leu^{18}	7.90	4.21	1.89, 1.75	γ 1.75, δ 0.95
Arg^{19}	8.03	4.19	2.00	γ_1 1.77, γ_2 1.86, δ 3.22, NH 7.26
Arg^{20}	8.03	4.26	2.00	γ_1 1.77, γ_2 1.86, δ 3.28, NH 7.28
Arg^{21}	7.95	4.12	1.93	γ_1 1.56, γ_2 1.72, δ 3.19, NH 7.23
Phe^{22}	8.14	4.44	3.19	aromatic 7.20, 7.38
Phe^{23}	8.27	4.43	3.22, 3.28	aromatic 7.38, 7.46
Leu^{24}	8.26	4.13	1.79	γ 1.61, δ 0.97
His^{25}	8.15	4.35	3.29	H_2 8.65, H_4 7.30
Lys^{26}	7.98	4.10	1.67, 1.88	γ 1.50, δ_1 1.23, δ_2 1.40, ε_1 2.69, ε_2 3.62, NH 8.05
Leu^{27}	7.90	4.00	1.61, 1.66	γ 1.67, δ_1 0.85, δ_2 0.90
Ile^{28}	7.37	3.90	1.82	γ_1 1.23, γ_2 1.55, γ_{CH_3} 0.85, δ_{CH3} 0.90
Ala^{29}	7.97	4.10	1.35	
Asp^{30}	8.12	4.75	2.70, 2.89	
Ile^{31}	7.62	4.07	1.89	γ_1 1.19, γ_2 1.54, $\gamma_{CH_3}+\delta_{CH_3}$ 0.85
His^{32}	8.44	4.84	3.24, 3.35	H_2 8.67, H_4 7.40
Thr^{33}	8.15	4.24	4.34	γ 1.28
Ala^{34}	8.35	4.33	1.43	

nm/min. The signal-to-noise ratio was improved by accumulating four to eight scans. The helix content of the peptides was determined according to the method of Greenfield and Fasman [14].

NMR Experiments

Two-dimensional ^{1}H-NMR spectra were recorded at 298 K without spinning on a Bruker Avance DMX-600 spectrometer. The data were processed on a Silicon Graphics workstation using the XWINNMR program. All NMR experiments were carried out in aqueous solution at 2.0 mM peptide in water at pH 4.5. TMS was used as the internal standard. All 2D DQFCOSY [15], CLEAN-TOCSY [16,17] and NOESY experiments were carried out in the phase-sensitive mode using the time proportional phase increment (TPPI) method [18], collecting 512 experiments of 2048 data points. Prior to Fourier transformation, the time-domain data were multiplied by $\pi/2-\pi/3$ shifted squared sine bell window functions in the F1 dimension and Gaussian window functions in the F2 dimension and zero-filled to 2048×1024 real points. The water peak was suppressed during the relaxation delay and, in the NOESY experiments, also during the mixing time. Baseline correction was performed after Fourier transformation, by a fifth-order polynomial function. CLEAN-TOCSY spectra were obtained with a mixing time of 70 ms; trim pulses were of 2.5 ms.

NOESY spectra were recorded using mixing times of 70, 120, 170, 200 and 220 ms, with a 5–10% random variation of the mixing period to reduce ZQ coherence contributions [19].

Structure Calculations

Inter-proton distances were calculated from the volumes of the integrated cross-peaks of the NOESY spectra at 200 ms mixing time, extracted from the NOE buildup curve, using the AURELIA software package. The calibration in the amide region was based on the sequential NH–NH cross peak originated from the interaction of amide protons of Gln^{16} and Asp^{17}, included in a well-defined helical segment, set to a distance of 2.8 Å. The calibration in the aliphatic region was based on the cross peak originated from the interaction of the geminal methylene protons of Asp^{30}, set to a distance of 1.8 Å. The upper and lower distance restraints were obtained by addition and subtraction of 10% of the calculated distance.

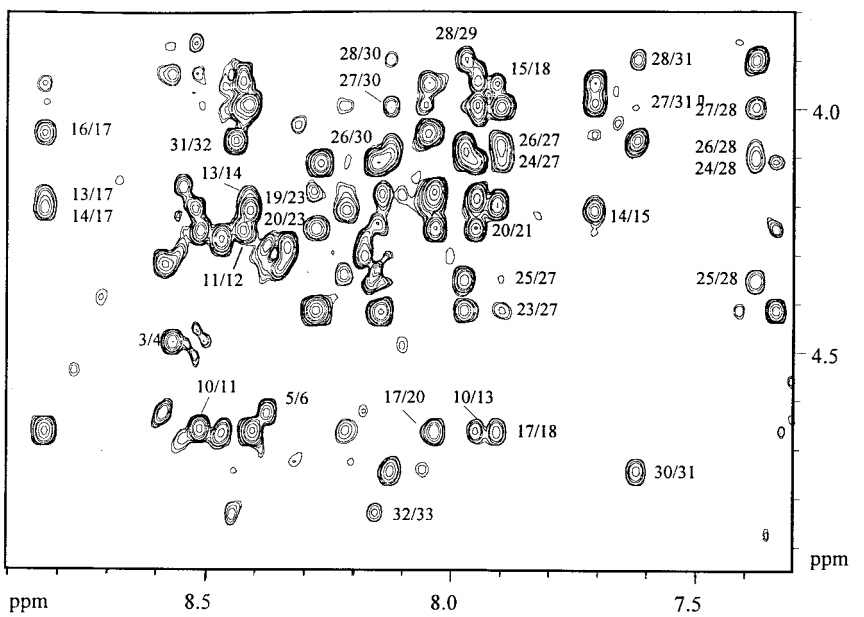

Figure 2 Fingerprint region of the NOESY spectrum at 600 MHz (200 ms mixing time) of the bis-lactam analog in water.

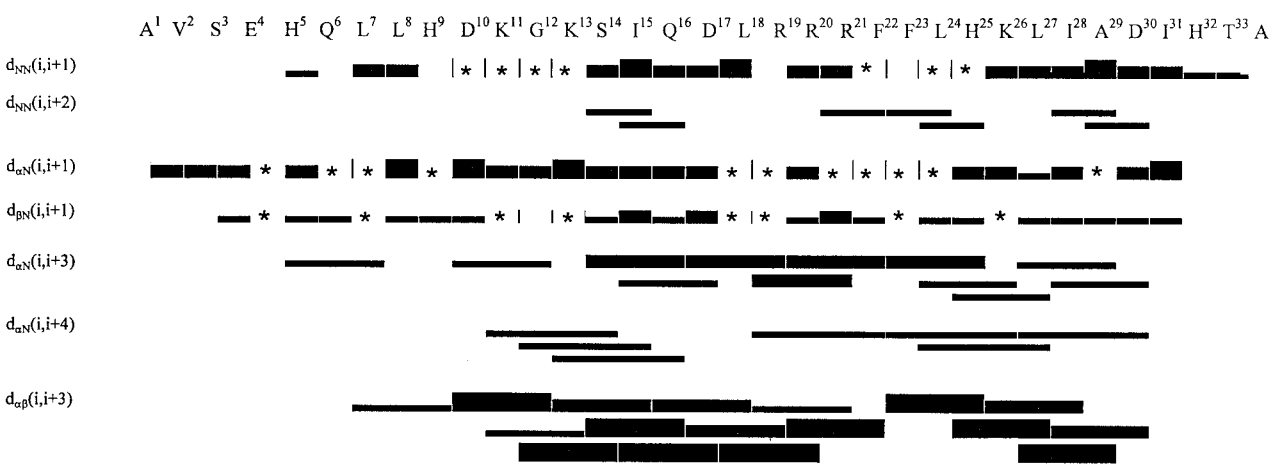

Figure 3 Summary of NOESY connectivities obtained in water. The NOEs are classified as strong (▭, $d < 3.0$ Å), medium (▯, $d < 4.0$ Å) and weak (▭, $d < 5.0$ Å). *, overlapped peak.

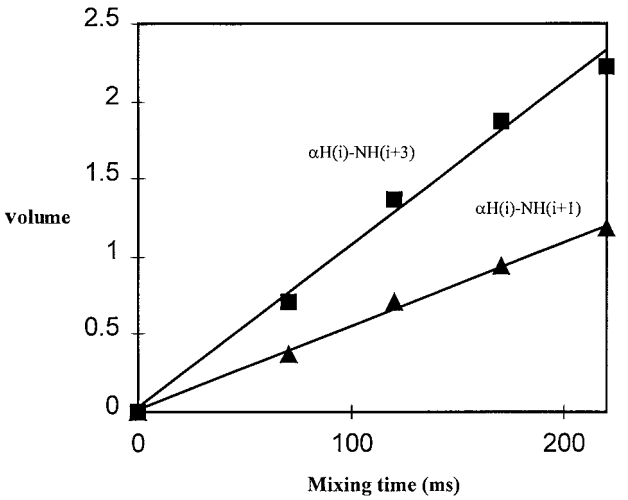

Figure 4 NOE build-up curve of NOESY cross peaks at different mixing times.

DG and MD calculations were carried out using the XPLOR 3.0 program [20]. From the DG protocol, 150 structures were generated and optimized by restrained MD calculations using the simulated annealing procedure. The detailed protocol was the following. Cycle I: (1) 20 ps of dynamics at 1500 K, with 10000 cycles, each one of 2 fs; (2) 30 ps of cooling from 1500 to 100 K (steps of 50 K), with 15000 cycles, each one of 2 fs; (3) 200 cycles of minimization. Cycle II: (1) warming at 1000 K and 25 ps cooling from 1000 to 100 K (steps of 50 K) with 25000 cycles, each one of 1 fs; (2) 200 cycles of minimization.

RESULTS

CD Results

The CD spectra of the peptide recorded in aqueous solution at pH 4.5 are shown in Figure 1. The spectrum is independent of peptide concentration in the range 1×10^{-5}–1×10^{-3} M. In contrast with the corresponding linear analog, the CD pattern indicates that the α-helix content, calculated according to the method of Greenfield and Fasman [14], is of the order of 40%. This result confirms the stabilizing effect of the i, $i+4$ lactam bridges on the α-helical structure.

NMR Results

The elements of secondary structure and their location along the sequence were determined by 2D NMR experiments. The assignment of proton resonances was achieved using standard procedures. In particular, all spin systems were identified using DQF-COSY and TOCSY spectra, while sequence specific assignments were performed using NOESY spectra. The complete assignment of all proton resonances is reported in Table 1. As an example, the fingerprint region of the NOESY spectrum is shown in Figure 2, where sequential and medium range connectivities are clearly evident. The summary of NOESY connectivities relevant for the assessment of secondary structure are shown in Figure 3. The resulting distances were placed in three different classes, with upper limits of 3.0, 4.0 and 5.0 Å, respectively. The NOE build-up curve is a linear function of the mixing time (Figure 4) and indicates that up to 220 ms mixing time there is no spin diffusion. Medium and short range connectivities (NH_i–NH_{i+1}, αH_i–NH_{i+3}, αH_i–NH_{i+4} and αH_i–βH_{i+3})

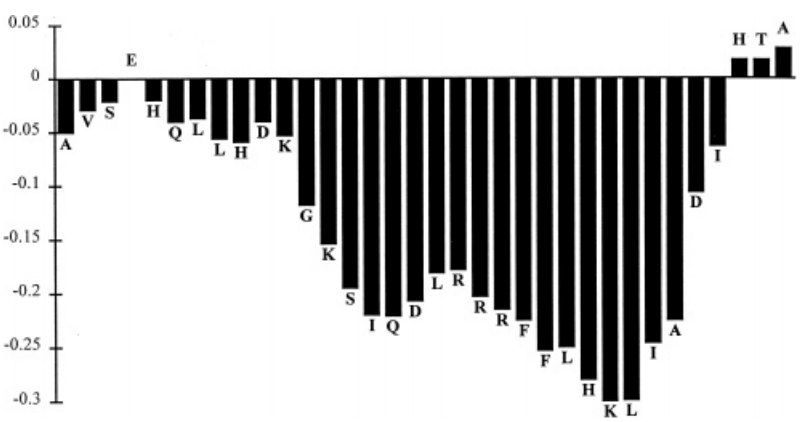

Figure 5 Chemical shift differences of αH protons in water.

Table 2 Average torsion angles (degree), with relative standard deviations, of the final lowest energy structures of the bicyclic lactam-constrained PTHrP-derived agonist in water

Residue	ϕ	ψ
Lys^{11}	-112 ± 36 (40)	-15 ± 21 (40)
Gly^{12}	-91 ± 23	-24 ± 8
Lys^{13}	-72 ± 9	-46 ± 20
Ser^{14}	-47 ± 14	-59 ± 13
Ile^{15}	-59 ± 9	-28 ± 3
Gln^{16}	-77 ± 4	-28 ± 8
Asp^{17}	-76 ± 6	-27 ± 3
Leu^{18}	-74 ± 7	-33 ± 17
Arg^{19}	-81 ± 21	-39 ± 22
Arg^{20}	-40 ± 2 (39)	-31 ± 3 (39)
Arg^{21}	-82 ± 5 (39)	-22 ± 31 (39)
Phe^{22}	-103 ± 35 (40)	-20 ± 11 (40)
Phe^{23}	-56 ± 16 (43)	-41 ± 24 (43)
Leu^{24}	-66 ± 19 (40)	-26 ± 4 (40)
His^{25}	-73 ± 6 (41)	-24 ± 7 (41)
Lys^{26}	-68 ± 13 (41)	-44 ± 19 (41)
Leu^{27}	-157 ± 18 (23)	$+40 \pm 11$ (23)
	-71 ± 22 (22)	-32 ± 6 (22)
Ile^{28}	-1 ± 24 (23)	-53 ± 17 (23)
	-68 ± 17 (22)	$+45 \pm 57$ (22)
Ala^{29}	-68 ± 15 (31)	$+31 \pm 11$ (31)
	$+44 \pm 2$ (11)	$+33 \pm 1$ (11)
Asp^{30}	-64 ± 18 (34)	-25 ± 17 (34)
	$+36 \pm 2$ (11)	$+36 \pm 5$ (11)

The averages are calculated over 45 structures except in cases where the values for some structures fell outside the $\pm 2\sigma$ range from the average. In those cases, the number of structures included in the average is indicated in parenthesis. Two sets of values are indicated when the structures clustered in two separate families. Here again, the number of structures included in each average is indicated in parenthesis. The average torsion angles of the first ten and the last four residues in the sequence are not reported because of the extremely high standard deviations.

indicate the presence of an α-helical segment spanning the sequence from D^{10} to I^{31}. No long range connectivity was observed between *N*-terminal and *C*-terminal segments of the molecule. The αH protons chemical shift differences with respect to the values of the random coil [21] are shown in Figure 5. Consistent with NOESY results, negative values higher than 0.1 ppm (typical of helical structure) are observed in the central part of the sequence from Gly^{12} to Asp^{30}. These data indicate that 19–22 out of 34 residues (56–65%) are present in the helical segment. The helix content is lower than that obtained by CD and NMR results in 1:1 H_2O/TFE (80%) [4], but higher than that obtained in water from the CD data reported above (40%). These results confirm that in aqueous solution the structure is more flexible than in the partially organic solvent system, and that there is a rapid exchange, on the NMR time-scale, among conformers with different helix content.

Structure Calculations

Integration of the NOESY spectra provided 299 conformationally informative constraints. By DG and subsequent structural refinement with MD calculations, 70 structures were obtained fulfilling the experimentally-derived inter-proton distances. The dihedral angles extracted from the 45 lowest energy structures are reported in Table 2. The minimum energy structure resulting from the MD protocol is shown in Figure 6. In all the low energy structures, two short helical segments are consistently present in the sequences 13–18 and 26–30, around the lactam bridges. The first helical turn is better defined than the second. This result is in agreement with the αH protons chemical shift differences in these portions of the sequence (Figure 5). The dispersion of the values of dihedral angles extracted from the 45 low energy structures indicates that the first ten and the last four residues are completely flexible. The standard deviations of the dihedral angles of the sequences 1–10 and 31–34 were so high that these residues were omitted from Table 2. In the region between the two helices, the preference for helical φ and ψ angles is maintained. However, the dispersion of the values of dihedral angles indicates flexibility at the level of Arg^{19} and in the sequence starting from Phe^{22} (Table 2). The standard deviations of φ and ψ dihedral angles is particularly relevant in the *C*-terminal portion of the helix (sequence 26–31) indicating flexibility despite the presence of the lactam bridge.

DISCUSSION

The characteristic structural motif, observed for PTH(1–34) and PTHrP(1–34) in H_2O/TFE and consisting of two *N*-terminal and *C*-terminal helical domains [3–10], is maintained in aqueous solution. The helical segments are located in the region around the lactam bridges. The most significant difference with respect to the results previously reported for the same analog in H_2O/TFE [4] is the substantially higher flexibility in aqueous solution.

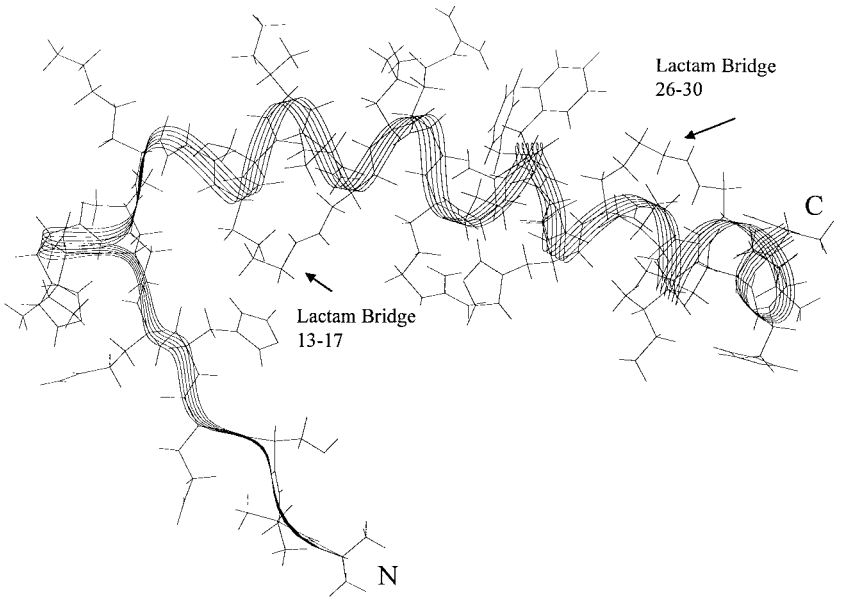

Figure 6 Lowest energy structure of the analog resulting from restrained MD calculations.

In H_2O/TFE, both CD and NMR data yielded an 80% helix content. In water, NMR data yielded a helix content in the range 56–65% against the 40% obtained by CD. The difference between the values obtained by CD and NMR is attributed to rapid exchange, on the NMR time-scale, among conformers with different helical contents. This is an indication that there is inherent flexibility of the sequence in the aqueous medium. This indication is further supported by the results of αH chemical shift differences (Figure 5) and by the dispersion of the dihedral angles extracted from the ensemble of the low energy structures. In fact, the first ten *N*-terminal and the last four *C*-terminal residues appear to be highly flexible (Table 2). In the central sequence 19–26, φ and ψ dihedral angles typical of the α-helical structure are observed in many of the low energy structures obtained by MD calculations. Thus, the conformational preference for α-helix in this sequence also is maintained, but with a high degree of flexibility.

Previous conformational studies of PTH/PTHrP-derived agonists and antagonists [4,5] and of PTHrP/PTH hybrids [22,23] indicated that flexibility points around positions 12 and 19, connecting helical segments, seem to be a biologically relevant structural motif in all potent (1–34) PTH and PTHrP analogs. From the results presented in this paper, we conclude that the essential features of secondary structure of the bis-lactam agonist, first observed in H_2O/TFE, are maintained in aqueous solution. In contrast, active and inactive linear analogs so far investigated were found to be mostly in an unordered conformation in aqueous solution. This result confirms the general stabilizing effect of the i, $i+4$ lactam bridges on α-helical structures.

Acknowledgements

The authors are indebted to Dr Dominga Deluca for preliminary NMR measurements. This work is supported, in part, by Grant R01-DK47940 (to M.R.) and by Consiglio Nazionale delle Ricerche (CNR), Biopolymer Research Center, University of Padova, Italy.

REFERENCES

1. Chorev M, Rosenblatt M. Structure-function analysis of parathyroid hormone and parathyroid hormone-related protein, in: *Parathyroids. Basic and Clinical Concepts*, J.P. Bilezikian, M.A. Levine and R. Marcus Eds., p. 139–156, Raven Press, New York, 1994.
2. Klaus W, Dieckmann T, Wray V, Schomburg D. Investigation of the solution structure of the human parathyroid hormone fragment (1–34) by ^{1}H NMR spectroscopy, distance geometry, and molecular dynamics calculations. *Biochemistry* 1991; **30**: 6936–6942.
3. Mierke DF, Maretto S, Schievano E, Deluca D, Bisello A, Rosenblatt M, Peggion E, Chorev M. Conformational

studies of mono- and bicyclic parathyroid hormone-related protein-derived agonists. *Biochemistry* 1997; **36**: 10372–10383.
4. Maretto S, Mammi S, Bissacco E, Peggion E, Bisello A, Rosenblatt M, Chorev M, Mierke DF. Conformational studies of mono- and bicyclic parathyroid hormone-related protein-derived antagonists. *Biochemistry* 1997; **36**: 3300–3307.
5. Neugebauer W, Surewicz WK, Gordon HL, Somorjai RL, Sung W, Willick GE. Structural elements of human parathyroid hormone and their possible relation to biological activities. *Biochemistry* 1992; **31**: 2056–2063.
6. Strikland LA, Bozzato RP, Kronis KA. Structure of human parathyroid hormone(1–34) in the presence of solvents and micelles. *Biochemistry* 1993; **32**: 6050–6057.
7. Wray V, Federau T, Gronwald W, Mayer H, Schomburg D, Tegge W, Wingender E. The structure of human parathyroid hormone from a study of fragments in solution using ^{1}H NMR spectroscopy and its biological implications. *Biochemistry* 1994; **33**: 1684–1693.
8. Barden JA, Cuthbertson RM. Stabilized NMR structure of human parathyroid hormone (1–34). *Eur J Biochem* 1993; **215**: 315–321.
9. Ray FR, Barden JA, Kemp BE. NMR Solution structure of the [Ala^{26}] parathyroid-hormone-related protein(1–34) expressed in humoral hypercalcemia of malignancy. *Eur J Biochem* 1993; **211**: 205–211.
10. Pellegrini M, Royo M, Rosenblatt M, Chorev M, Mierke DF. Addressing the tertiary structure of human parathyroid hormone (1–34). *J Biol Chem* 1998; **273**: 10420–10427.
11. Bisello A, Nakamoto C, Rosenblatt M, Chorev M. Mono- and bicyclic analogs of parathyroid hormone-related protein. 1. Synthesis and biological studies. *Biochemistry* 1997; **36**: 3293–3299.
12. Chorev M, Roubini E, McKee RL, Gibbons SW, Caulfield MP, Rosenblatt M. Cyclic parathyroid hormone-related protein antagonists. Lysine 13 to aspartic acid 17 [*i*, to (*i* + 4)] side-chain to side-chain lactamization. *Biochemistry* 1991; **30**: 5968–5974.
13. Maretto S, Schievano E, Mammi S, Bisello A, Nakamoto C, Rosenblatt M, Chorev M, Peggion E. Conformational studies of a potent Leu^{11}, D-Trp^{12}-containing lactam-bridged parathyroid hormone-related protein-derived antagonist. *J Pept Res* 1998; **52**: 241–248.
14. Greenfield N, Fasman GD. Computed circular dichroism spectra for the evaluation of protein conformation. *Biochemistry* 1969; **8**: 4108–4116.
15. Rance M, Sørensen OW, Bodenhausen G, Wagner G, Ernst RR, Wüthrich K. Improved spectral resolution in COSY proton NMR spectra of proteins via double quantum filtering. *Biochem Biophys Res Commun* 1983; **117**: 479–485.
16. Bax A, Davis DG. MLEV-17-based two-dimensional homonuclear magnetization transfer spectroscopy. *J Magn Reson* 1985; **65**: 355–360.
17. Griesinger C, Otting G, Wüthrich K, Ernst RR. Clean TOCSY for ^{1}H spin system identification in macromolecules. *J Am Chem Soc* 1988; **110**: 7870–7872.
18. Bodenhausen G, Vold RL, Vold RR. Multiple quantum spin-echo spectroscopy. *J Magn Reson* 1980; **37**: 93–106.
19. Macura S, Huang Y, Suter D, Ernst RR. Two-dimensional chemical exchange and cross-relaxation spectroscopy of coupled nuclear spins. *J Magn Reson* 1980; **43**: 259–281.
20. Brunger AT. *X-PLOR Manual (version 3.0)*, Yale University, CT, USA, 1992.
21. Pastore A, Saudek V. The relationship between chemical shift and secondary structure in proteins. *J Magn Reson* 1990; **90**: 165–176.
22. Peggion E, Mammi S, Schievano E, Garbin E, Behar V, Rosenblatt M, Chorev M. Conformational studies of parathyroid hormone (PTH)/PTH-related protein (PTHrP) segmental hybrid peptides. *Biochemistry* 1999 (manuscript in preparation).
23. Peggion E, Mammi S, Schievano E, Behar V, Rosenblatt M, Chorev M. Conformational studies of parathyroid hormone (PTH)/PTH-related protein (PTHrP) point-mutated hybrids. *Biopolymers* 1999 (in press).

